Sick-Bird Syndrome: The Operational Imperative for pLEO Debris Mitigation

Kenny Grosselin[1] and Zach Hughes[2]

[1]Secretary of Defense Strategic Thinkers Program, kenneth.grosselin.2@us.af.mil
[2]School of Advanced Warfighting, zachary.hughes.3@us.af.mil

ABSTRACT

The U.S. military is investigating the utility of proliferated low Earth orbit (pLEO) satellite architectures. Because pLEO achieves global coverage through hundreds or thousands of small satellites, it promises many important military advantages. But the relationship between military pLEO applications and orbital debris is largely unresearched. Our paper examines how orbital debris will impact pLEO operations and how pLEO architectures will contribute to debris growth across the space domain. To do this, we use a system of differential equations to model the local and regime-wide evolution of orbital debris. The model assesses local impacts to constellation availability based on collisions and collision avoidance maneuvers as well as regime-wide trends in the total debris population. This analysis shows lackadaisical mitigation for military pLEO architectures can have a deleterious effect on constellation availability in as little as five years after full operational deployment. Given these findings, military pLEO architectures will likely need to adhere to debris mitigation practices that are stricter than the minimum specifications in U.S. Government (2019) Orbital Debris Mitigation Standard Practices.

INTRODUCTION

Proliferated low Earth orbit (pLEO)—defined as a constellation with hundreds or thousands of low Earth orbit (LEO) satellites—is an emerging design architecture for military space missions. It promises several important military advantages. PLEO proponents claim that operating from a low altitude can significantly reduce connectivity latency as compared to medium Earth orbit or geosynchronous Earth orbit (Space Development Agency, 2020). Additionally, because pLEO constellations involve hundreds or thousands of satellites, the overall system is resilient to individual satellite disruptions. This graceful degradation makes pLEO more survivable in a contested or operationally limited environment. Furthermore, manufacturing hundreds or thousands of small satellites, as opposed to a few exquisite systems, could offer economies of scale and make space systems more cost effective and more responsive to new requirements and technologies.

https://doi.org/10.5711/1082598327283

APPLICATION AREA:
Operational Contribution of Space Systems

OR METHOD:
Forecasting/Time Series Analysis

These potential benefits have ignited a flurry of commercial and military research. The Defense Advanced Research Projects Agency (DARPA) "Blackjack" program aims to demonstrate pLEO technology on orbit by the end of 2021. Additionally, the Space Development Agency (SDA) has solicited bids for a pLEO system with satellites at 600 kilometers (km), 1,000 km, and 1,200 km. This multilayer architecture would include a mix of communication payloads and remote sensing capabilities. SDA's first 20 satellites are scheduled to launch in 2022.

Despite this enthusiasm, the relationship between pLEO and orbital debris remains largely uninvestigated in a military context. Congestion is a growing threat to all satellite operations in low Earth orbit. It seems obvious that military pLEO constellations will impact the growth of orbital debris and orbital debris will impact the deployment and employment of pLEO constellations. But a detailed understanding of this bidirectional relationship must inform the development, acquisition, operation, and disposal of military pLEO capabilities. Unfortunately, published research on this topic is scarce.

In this paper, we examine the bidirectional relationship between orbital debris and proposed military pLEO architectures. To do this, we specify a system of differential equations that models the local and regime-wide evolution of orbital debris. Our model uses previously validated parameters for collision probabilities and debris generation. We then explore how notional pLEO architectures and potential alternatives for debris mitigation impact constellation availability and the long-term growth of debris. Based on these results, we recommend specific system requirements for future pLEO military architectures.

LITERATURE REVIEW

Orbital debris is a byproduct of human activity in space. Colloquially referred to as space junk, orbital debris includes large objects such as used rockets and derelict satellites, small objects such as nuts, bolts, and camera lenses, and miniscule objects such as chips of paint and frozen propellant chemicals. Like all objects in orbit, debris sustains tremendous speeds—faster than 7 km/second (s) in LEO. At these energies, even a 1 centimeter (cm) aluminum fragment can catastrophically destroy an operational satellite. Collisions also perpetuate a vicious cycle. Every collision creates more debris, which in turn increases the frequency of future collisions. A piece of debris will persist in orbit until its trajectory decays into the atmosphere and the object disintegrates under the massive heat created during reentry. Reentry timelines depend on altitude and can range from days (altitudes less than 400 km) to years (400–500 km) to decades (500–700 km) to even centuries (greater than 900 km) (Reesman et al., 2020).

Orbital debris flux—defined as expected collision rate per unit of surface area—is central to all orbital debris models. Because flux is a rate, orbital debris models typically use exponential distributions to quantify collision probabilities and differential equations to forecast debris growth over time (Kessler and Cour-Palais, 1978). More complicated models incorporate three-dimensional geometry, orbital propagation, atmospheric drag, solar activity, and radiation pressure (Kessler et al, 1996; Liou et al., 2004; Krisko, 2007; Bradley and Wein, 2009). While spatial debris flux dominates the probability of collision calculation, other factors such as average relative velocity and exposed cross section abet a measurable impact on collision frequency (McKnight and Anz-Meador, 1993). Orbital debris models also vary in scope. Micro-level orbital debris models examine a small segment of outer space, usually a spherical shell or an orbit of interest. Macro-level models, in contrast, evaluate the dynamics of orbital debris across a larger region, typically LEO, MEO, GEO, or the complete volume of geocentric space.

Kessler and Cour-Palais (1978) were the first to model collision probabilities based on orbital motion. Debris hazard was minimal at the time; however, Kessler and Cour-Palais showed how the self-regenerative nature of the debris population could accelerate the collision hazard as human activity in outer space increased. NASA's empirical research validated these models and confirmed the self-propagating nature of space debris (Kessler, 1981; Su and Kessler, 1985). These findings motivated the hypothesis that collisional cascading would eventually surpass human

activity as the largest source of debris growth (Su, 1986; Eichler and Rex, 1990; Kessler, 1991). In 2006, Liou and Johnson (2006) showed that the debris population in LEO had reached this critical tipping point. Collisions, not human activity, had become the dominant source of future debris in LEO.

Congestion's dire consequences were dramatically demonstrated on February 10, 2009, when a defunct Russian Cosmos military satellite collided with an active commercial satellite owned by Iridium Communications—an event referred to as the Cosmos-Iridium satellite collision. The collision destroyed both satellites and created 2,000 new pieces of debris larger than 10 cm (Weeden, 2014). But orbital congestion's deleterious impacts extend beyond the dramatic. As debris increases, direct and indirect costs accrue to satellite operators in the form of increased collision risk, service interruptions, and the costs associated with satellite hardening, satellite maneuverability, and satellite collision avoidance monitoring.

The various strategies for debris curtailment divide into three general categories: reactive collision avoidance (COLA), active debris removal, and passive debris mitigation.

Reactive COLA is a helpful but imperfect solution. Maneuverable spacecraft can conduct evasive maneuvers to avoid collisions (Kim and Paté-Cornell, 2019). But COLA is only viable when a maneuverable satellite is involved in a forecasted collision. Avoidance maneuvers are infeasible when the colliding objects are unmaneuverable or inoperable. These collisions may not directly result in the destruction of a satellite, but they generate new debris that increases the overall debris risk. COLA is also only effective for predicted collisions. Space traffic management (STM) sensors cannot reliably track objects in LEO smaller than 10 cm (Liou, 2020). This creates a precarious blind spot—objects between 1 cm and 10 cm are simultaneously large enough to destroy a satellite but too small to be reactively avoided. According to NASA's Orbital Debris Engineering Model and in situ sampling, in LEO this hidden debris population is 21 times larger than the trackable population (NASA, 2020). COLA maneuvers also result in a temporary mission outage. Post-maneuver mission loss for LEO satellites ranges from 15 minutes to 24 hours based on satellite performance and mission context. Because of this mission loss, frequent COLA maneuvers can diminish constellation availability.

Active debris removal (ADR), also referred to as debris remediation, aims to remove existing space debris from LEO, especially large objects whose fragmentation would generate massive new debris fields. There is a near-consensus within the debris research community that remediation is necessary for the long-term stabilization of orbital debris (Liou, 2011; White and Lewis, 2014; Weeden, 2017). Unfortunately, the technology associated with ADR is immature and unproven. Proposals exist, but none have been demonstrated on a viable scale. Scientists and engineers must first demonstrate practical end-to-end technology for debris removal before remediation can be a dependable policy alternative.

Passive mitigation aims to minimize the creation of new orbital debris by modifying how satellites are designed, operated, and disposed. Some satellites shed components, for example, lens caps or fastening bolts, during routine operations. A responsibly designed satellite mitigates the creation of orbital debris by minimizing the number of untethered components on a satellite. Because satellites can remain in LEO for decades or centuries before falling back to Earth, many of the most effective mitigation measures occur after a satellite has completed its operational mission. During post-mission disposal (PMD) activities, satellite operators vent pressurized containers and maneuver a satellite into a disposal orbit. In LEO, this involves lowering the altitude of a satellite to hasten reentry. A defunct satellite that quickly reenters Earth's atmosphere has fewer collision opportunities and is thus less likely to contribute to debris growth. Satellite reliability also plays an important role in mitigating orbital debris. A satellite malfunction may prevent operators from properly disposing of a satellite, confining the now defunct vehicle to LEO for decades or centuries.

U.S. Orbital Debris Mitigation Standard Practices (ODMSP) stipulate orbital debris mitigation guidelines for all civil, commercial, and military U.S. satellite programs. Approved by the

National Space Council, ODMSP stipulates that LEO satellites reenter Earth's atmosphere no later than 25 years after completion of mission (25-year PMD). Furthermore, satellites must be designed with enough reliability to achieve 90% compliance with the 25-year PMD timeline, though ODMSP recommends 99% compliance for pLEO architectures. In practice, only 50%–60% of LEO satellites comply with the 25-year PMD timeline (ESA, 2019; Weeden, 2020).

Investigating the relationship between pLEO and orbital debris is a nascent avenue of inquiry with two distinct branches. The first branch investigates how pLEO architectures will impact congestion in the space environment (Virgili et al., 2016; Lewis et al., 2017; Henning, 2019). Unsurprisingly, pLEO architectures will drastically accelerate the accumulation of orbital debris. COLA, strict mitigation, and active debris removal can reduce the growth rate, but efficacy depends on the constellation under consideration. The second branch is less developed than the first and investigates the risk orbital debris poses to pLEO architectures (Swinerd et al., 1999; Radtke et al., 2017). Orbital debris threatens all LEO satellites; pLEO satellites are no different. While the risk probabilities are clear, the practical implications are less so. Large numbers of satellite increase the risk for any single operator, but also create opportunities for the graceful degradation of satellite services should a collision occur. Noticeably absent from the literature is any assessment of the impact that orbital debris will have on the availability of pLEO architectures.

From a military perspective, significant gaps exist in both branches. Published research exclusively focuses on commercial constellations. Military pLEO architectures differ from their commercial counterparts in both form and function. Projecting debris growth and calculating risk probabilities are not enough. PLEO architectures must be scrutinized in the context of military applications and accepted measures of performance. Furthermore, commercial companies generally operate in a small subset of LEO. This allows researchers to assess local collision risks separate from regime-wide impacts to the LEO environment. The U.S. national security space enterprise, in contrast, operates from a diverse set of orbits. Regime-wide impacts and local collision risk must be assessed as interrelated consequences of pLEO architectures. The results of such analysis can then inform the design, procurement, operation, and disposal of military pLEO architectures.

MODEL FORMULATION

Our model partitions LEO into N concentric spherical shells indexed in $n \in \{1,2,3,\ldots,N\}$ from lowest to highest. Each has a constant thickness of Δh meters. Four types of objects exist in each shell, $\Gamma \in \{O,D,L,H\}$: operational satellites (O), derelict satellites that are intact but inoperable (D), debris fragments large enough to reliably track and evade (L), and hidden objects large enough to destroy operational satellites but too small for space traffic management censors to reliably track (H). Let $O_n(t)$ represent the number of operational satellites in the nth orbital shell at time t. Similarly, $D_n(t)$, $L_n(t)$, and $H_n(t)$ represent the population count of derelict, large, and hidden objects, respectively. Four overriding processes govern the evolution of this system: operational satellites are launched, operational satellites become derelict after end-of-life disposal, derelict satellites, and debris fragments decay back to Earth, and orbital collisions create new fragments of debris.

Understanding orbital collisions is the proximal objective of the overall model. Collision hazard varies with debris density in each spherical shell. By assuming objects are uniformly distributed in each shell, the density of object $\Gamma \in \{O,D,L,H\}$ in the nth shell at time t is expressed as the total number of objects divided by the volume of the spherical shell:

$$d_{n,\Gamma} = \frac{\Gamma_n(t)}{\frac{4}{3} \cdot \pi \cdot \left[(r_\oplus + h_n + \Delta h)^3 - (r_\oplus + h_n)^3\right]}. \quad (1)$$

In Equation (1), $r_\oplus$ is the average radius of Earth and h_n is the lower altitude of the nth shell.

Debris flux (F) is defined as the expected debris impact rate per unit of surface area and is the product of spacecraft velocity, nominally meters per second (m/s) and average orbital density (nominally #objs/m^3):

$$F_n = v_n \cdot d_n \,. \tag{2}$$

Because our model assumes circular orbits, all objects maintain a constant velocity along their orbital path (Wertz and Larson, 1999):

$$v_n = \sqrt{\frac{\mu_\oplus}{r_\oplus + h_n}}. \tag{3}$$

In this expression, $\mu_\oplus$ represents the standard gravitational parameter for Earth (3.986×10^{14} m^{3}s^{-2}).

Multiplying flux by the collision surface area yields the expected number of collisions for a specific object. This rate is then scaled across the entire population for each collision type. Thus, the passive collision rate between object types $\Gamma \in \{O,D,L,H\}$ and $\Upsilon \in \{O,D,L,H\}$ in the nth orbital shell, denoted $C_{n,\Gamma,\Upsilon}$, is expressed as follows:

$$C_{n,\Gamma,\Upsilon} = v_n \cdot d_{n,\Gamma}(t) \cdot \Upsilon_n(t) \cdot \pi \cdot (r_\Gamma + r_\Upsilon)^2 \qquad \Gamma, \Upsilon \in \{O,D,L,H\}. \tag{4}$$

In Equation (4), r_Γ and r_Υ represent the radii of objects $\Gamma \in \{O,D,L,H\}$ and $\Upsilon \in \{O,D,L,H\}$, respectively. Assuming all objects are spheres, the term $\pi \cdot (r_\Gamma + r_\Upsilon)^2$ in Equation (4) represents the combined collision area of two objects (Kessler et al., 1996). Substituting (1) into (4) yields a population-based estimate of the passive collision rate between two different categories of objects:

$$C_{n,\Gamma,\Upsilon} = \frac{3 \cdot v_n \cdot \Gamma_n(t) \cdot \Upsilon_n(t) \cdot (r_\Gamma + r_\Upsilon)^2}{4 \cdot \left[(r_\oplus + h_n + \Delta h)^3 - (r_\oplus + h_n)^3\right]} \; \Gamma, \Upsilon \in \{O,D,L,H\}. \tag{5}$$

Note that Equation (5) implies that $C_{n,\Gamma,\Upsilon} = C_{n,\Upsilon,\Gamma}$. This symmetry makes intuitive sense—every collision involves a pair of objects. Of course, Equation (5) is a passive collision rate. Space traffic management allows maneuverable satellites to evade predicted collisions. Since derelict satellites and large debris fragments are reliably tracked throughout LEO, our model assumes that operational satellites only collide with hidden debris fragments. All other pairwise collisions are possible, with Equation (5) determining the appropriate rate.

Every collision creates and destroys debris. Colliding objects are destroyed, but the collision produces new large and hidden fragments. Said differently, collisions subtract from the operational and derelict population but increase the number of large and hidden debris fragments. As an example, consider a collision between a derelict satellite and a large debris fragment. The derelict is destroyed, which reduces the population of derelict satellites by one. The large fragment is also destroyed in this notional example, but it is replaced by new debris fragments generated in the collision, along with new hidden debris fragments. The result is a net decrease in derelicts but a net increase in large and hidden fragments. To model this process, we introduce two new variables. Let $G_{n,\Gamma}$ represent the collision induced rate of change of population $\Gamma \in \{O,D,L,H\}$ in the nth spherical shell and the scalar $\delta_{\Theta,\Gamma,\Upsilon}$ express the average net increase in fragments of type $\Theta \in \{L,H\}$ generated when objects of type $\Gamma \in \{O,D,L,H\}$ and type $\Upsilon \in \{O,D,L,H\}$ collide. Our assumptions yield the following four expressions:

$$G_{n,O} = -C_{n,O,H}, \tag{6}$$

$$G_{n,D} = -(2 \cdot C_{n,D,D} + C_{n,D,L} + C_{n,D,H}), \tag{7}$$

$$G_{n,L} = \delta_{L,O,H} \cdot C_{n,O,H} + \delta_{L,D,D} \cdot C_{n,D,D} + \delta_{L,D,L} \cdot C_{n,D,L} + \delta_{L,D,H} \cdot C_{n,D,H} + \delta_{L,L,L} \cdot C_{n,L,L} + \delta_{L,L,H} \cdot C_{n,L,H}, \tag{8}$$

$$G_{n,H} = \delta_{H,O,H} \cdot C_{n,O,H} + \delta_{H,D,D} \cdot C_{n,D,D} + \delta_{H,D,L} \cdot C_{n,D,L} + \delta_{H,D,H} \cdot C_{n,D,H} + \delta_{H,L,L} \cdot C_{n,L,L} + \delta_{H,L,H} \cdot C_{n,L,H} + \delta_{H,H,H} \cdot C_{n,H,H}. \tag{9}$$

Equations (6) and (7) reflect that collisions destroy operational and derelict satellites, while Equations (8) and (9) capture the assumption that collisions result in a net increase in the large and hidden fragment populations. Furthermore, Equation (6) expresses the assumption that operational satellites only collide with hidden fragments; STM allows operational satellites to evade all other collisions. Equation (7) reflects that a collision between two derelict satellites decrements the derelict population by 2. Finally, because mass is conserved, a collision between two hidden fragments does not produce any large fragments. Thus, we omit the term $\delta_{L,H,H} \cdot C_{n,H,H}$, since $\delta_{L,H,H} = 0$.

Equation (5) can also be modified to describe the frequency of collision avoidance maneuvers ($COLA_{n,O,\Upsilon}$) given a projected miss distance (μ_n) that triggers an evasive maneuver:

$$COLA_{n,O,\Upsilon} = \frac{3 \cdot v_n \cdot O_n(t) \cdot \Upsilon_n(t) \cdot (r_O + r_\Upsilon + \mu_n)^2}{4 \cdot \left[(r_\oplus + h_n + \Delta h)^3 - (r_\oplus + h_n)^3 \right]} \; \Upsilon \in \{D, L\}. \tag{10}$$

In addition to debris generating collisions, other processes impact the dynamics of the system. Operational satellites are launched into each shell at rate $\varphi_n(t)$ and retired at rate $\phi_n(t)$. Over time, passive objects (i.e., *D*, *L*, and *H*) decay into lower shells and eventually transition out of the system. Operational satellites become derelict satellites after end-of-life passivation. Disposals successfully occur with reliability θ based on the design characteristics of the system. Objects that fail PMD persist as defunct satellites in their operational orbit until atmospheric drag lowers their altitude. With the proper technology, derelict satellites can be actively removed from critical orbital regimes at a constant rate, α, to help remediate long-term collision hazard in key orbits. Post-mission reliability, disposal altitude, and active debris removal represent important policy levers for further consideration.

Our goal is to illustrate how post-mission reliability (θ_n), post-mission disposal altitude $(\rho \in \{1, 2, 3, \ldots, N\})$, and active debris removal rate (α_n) impact local orbital congestion, constellation availability, and LEO-wide debris accumulation. Because we wish to explore a broad policy space over an intergenerational time horizon (50–100 years), we use ordinary differential equations to model the long-term evolution of the system.

MODEL SPECIFICATION

The following parameters are used throughout the model:

- t: Time
- $n, m \in \{1, 2, 3, \ldots, N\}$: Index of spherical shells
- $O_n(t)$: Operational satellite population in n at t
- $D_n(t)$: Derelict satellite population in n at t
- $L_n(t)$: Large (trackable) debris fragment population in n at t
- $H_n(t)$: Hidden (untrackable) debris fragment population in n at t
- $\varphi_n(t)$: Satellite launch rate into n at t
- $\phi_n(t)$: Satellite retirement rate in n at t
- $\beta_n(t)$: Passive decay rate in n at t
- $C_{n,\Gamma,\Upsilon}$: Collision rate between Γ and Υ in n, reference Equation (5)

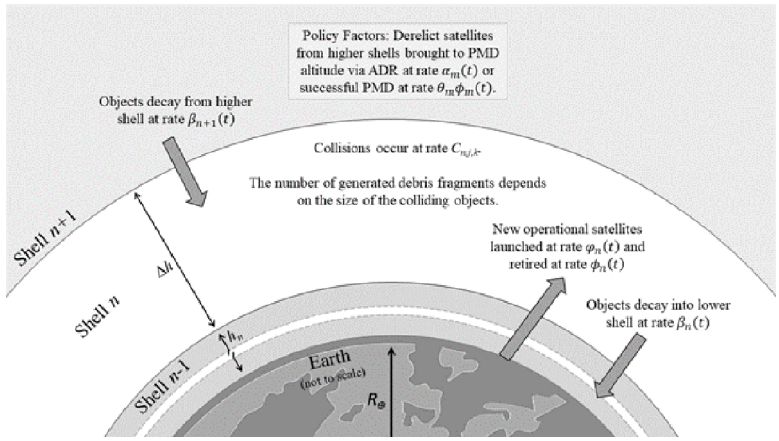

Figure 1. Visual depiction of model.

- $\delta_{\Theta,\Gamma,\Upsilon}$: Net increase in the number of fragments of type Θ generated when types Γ and Υ collide
- $G_{n,\Gamma}$: Collision induced rate of change of population $\Gamma \in \{O,D,L,H\}$ in the nth spherical shell, reference Equations (5)–(9)
- θ_n: Post-mission disposal reliability in n
- $\rho \in \{1, 2, 3, \ldots, N\}$: Post-mission disposal altitude block
- $\alpha_n(t)$: Active debris removal rate in n at t

Using this notation, and the equations derived in (1)–(10) yields the following system of ordinary differential equations:

$$\frac{dO_n}{dt} = \varphi_n(t) - \phi_n(t) + G_{n,O}, \tag{11}$$

$$\frac{dD_n}{dt} = (1-\theta_n)\cdot\phi_n(t) + \beta_{n+1}(t)\cdot D_{n+1} - \beta_n(t)\cdot D_n - \alpha_n(t) + G_{n,D} \text{ for } n > \rho, \tag{12}$$

$$\frac{dD_n}{dt} = \phi_n(t) + \beta_{n+1}(t)\cdot D_{n+1} - \beta_n(t)\cdot D_n + G_{n,D} \text{ for } n < \rho, \tag{13}$$

$$\frac{dD_n}{dt} = \phi_n(t) + \beta_{n+1}(t)\cdot D_{n+1} - \beta_n(t)\cdot D_n + G_{n,D} + \sum_{m\in\{\rho+1,\ldots,N\}} \alpha_m(t) + \theta_m\cdot\phi_m(t) \text{ for } n = \rho, \tag{14}$$

$$\frac{dL_n}{dt} = \beta_{n+1}(t)\cdot L_{n+1} - \beta_n(t)\cdot L_n + G_{n,L}, \tag{15}$$

$$\frac{dH_n}{dt} = \beta_{n+1}(t)\cdot H_{n+1} - \beta_n(t)\cdot H_n + G_{n,H}. \tag{16}$$

Figure 1 illustrates the geometry of the model. Equations (12), (13), and (14) enforce PMD disposal conditions. Disposal maneuvers are not required for operational satellites below the PMD altitude standard ($n < \rho$). These satellites are already at an altitude that ensures PMD compliance. Satellites above the PMD altitude ($n > \rho$) are relocated to the disposal altitude (ρ) with reliability θ_n. When disposal fails $(1-\theta_n)$, the derelict satellite remains in its operational shell.

Table 1. Four notional p-LEO constellations.

	Altitude (km)	Satellites (#)	Single satellite 20° access ($10^6 \times km^2$)	Total access ($10^6 \times km^2$)	Design life (years)	Launch rate (satellites/year)
Low	600	840	4.5	~3,800	4	210
Medium-low	800	547	7.0	~3,800	4	137
Medium-high	1,000	400	9.5	~3,800	4	100
High	1,200	312	12.2	~3,800	4	78

Because active debris removal is still an immature technology, the analysis that follows sets $\alpha_n = 0$ for all considered scenarios; however, the parameter is included to support future analysis.

MODEL PARAMETERIZATION

Our parameterization starts at an altitude of 300 km and segments LEO into 35 spherical shells, each with a Δh of 50 km. Tracking the evolution of $\Gamma \in \{O,D,L,H\}$ in each shell yields a system of 140 ordinary differential equations.

We model four comparable pLEO constellations, listed in Table 1. These four constellations approximate the pLEO designs Department of Defense (DOD) organizations have proposed. To facilitate comparisons, the total instantaneous access area of each constellation is approximately equal. This makes them roughly comparable based on Earth coverage and total field-of-view. All else being equal, higher constellations can provide the same amount of Earth coverage with fewer satellites. Based on design specifications for SDA's initial pLEO system, we assume satellites have a four-year design life (Space Development Agency, 2020). Thus, each year 25% are replenished and 25% retire.

In addition to these four notional pLEO constellations, we also model nominal satellite activity across LEO. Where possible, we use relationships and parameters validated in real-world or laboratory experiments (Polk and Roebuck, 2015). Where validated relationships are not available, we use conservative estimates that understate the scope and scale of debris generation. Launch activity is modeled as the sum of the historical launch rates (Lewis, 2019) and the notional pLEO launch activity in Table 1. The initial population of operational satellites in each altitude band is based on estimates from the USSPACECOM satellite catalog, while NASA's Orbital Debris Engineering Model provides the initial population of orbital debris in each altitude band (see Figures 2 and 3). Satellite decay rate, $\beta_n(t)$, decreases with altitude and varies with the 11-year solar cycle (Reesman et al., 2020).

Based on regulatory filings for commercial pLEO constellations, we assume all operational and defunct satellites have a maximum diameter of 8 meters and a mass of 386 kilograms (kg) (Space Exploration Technologies Corporation, 2016). We model large debris fragments with a diameter of 10 cm and hidden debris fragments with a diameter of 1 cm. Because 10 cm and 1 cm represent the lower boundary of the L and H populations based on contemporary space surveillance sensor performance, this parameterization expresses a conservative estimate of the frequency and severity of debris collisions.

We use NASA's parametric relationships for collision fragmentation to estimate $\delta_{\Theta,\Gamma,\Upsilon}$ (Johnson et al., 2001). This research models two types of collisions. Catastrophic collisions involve the total fragmentation of both objects while noncatastrophic collisions are primarily characterized by fragmentation of the smaller object and cratering of the larger object. Based on these findings, we model any collision where both objects are type O, D, or L as catastrophic (NASA, 2020). All other collisions (specifically, all collisions involving a hidden piece of debris) are modeled as noncatastrophic.

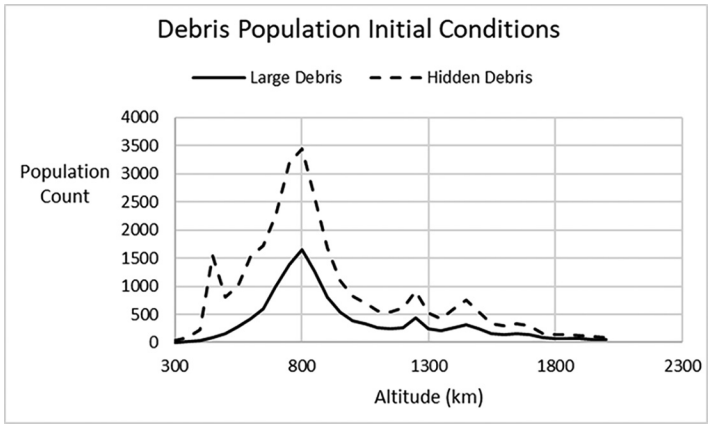

Figure 2. Initial debris population.

When two objects with mass m_1 and m_2 (in kilograms) are involved in a catastrophic collision, the expected number of new debris fragments larger than l_c (in meters) corresponds to the following power law distribution:

$$P(l_c) = 0.1 \cdot (m_1 + m_2)^{0.75} \cdot l_c^{-1.71}. \tag{17}$$

When two objects are involved in a noncatastrophic collision, the term $m_1 + m_2$ in Equation (17) is replaced by the product of the smaller objects mass and the collision velocity. Thus, Equation (17) is used to calculate the number of large fragments (greater than 10 cm) and hidden fragments (between 1 cm and 10 cm) a collision type generates. All velocity calculations are based on the orbit where the collision occurs, as modeled in Equation (3). All mass calculations assume a spherical volume at the density of aluminum. For example, Equation (17) predicts that a collision between a 386 kg derelict satellite and a 10 cm piece of aluminum debris generates approximately 449 large pieces of debris. The net impact is 448 large pieces of debris added to the local environment (449 new pieces minus the one piece destroyed in the collision).

A shortcoming of our model is that it assumes all satellites and debris follow a circular path around Earth. While orbit eccentricity for operational satellites depends on mission requirements, to date, all proposed DOD and commercial pLEO constellation rely on circular orbits to achieve uniform coverage. Debris fragments may also follow noncircular orbits; however, as is done elsewhere in the literature, the estimates for debris flux initial conditions for each shell incorporate

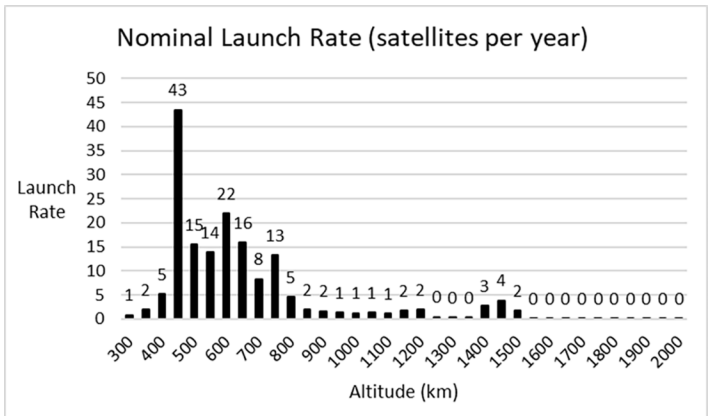

Figure 3. Nominal satellite launch activity.

debris in elliptical orbits by using a time-based weighting process that accounts for the fraction of time spent in each shell (Bradley and Wein, 2009). Another shortcoming is that the model treats all derelict spacecraft as the same size. Any large derelict vehicle involved in a collision, especially any massive upper stage rocket bodies that remain in orbit, will have an outsized environmental impact.

RESULTS

Constellation Availability

We first explore how PMD reliability impacts constellation availability. We define constellation availability as the expected proportion of operational satellites in the constellation. Our definition of constellation availability does not include built-in system redundancy and is thus different from mission availability. Determining what constitutes an acceptable lower bound on constellation availability is a matter of judgment. Acceptable availability will depend on quantitative factors such as the amount of overlapping coverage in the constellation as well as qualitative factors such as the risk tolerance for a specific mission area. For example, the same availability threshold may be acceptable for satellite communication services but unacceptable for missile warning activities. Because we expect availability to decrease over time as debris accumulates in the spherical shell of interest, time horizon is also a factor. In the context of military operations, a constellation that maintains acceptable availability for only a portion of its intended design life is ultimately unacceptable. While cognizant of these context-specific factors, the remainder of this paper uses an availability of 0.9 after 25 years as the threshold of acceptability. A 25-year time horizon may seem like the distant future until one considers that the Global Positioning System (GPS) was designated fully operational in 1995—over 25 years ago.

Every satellite that fails before disposal persists as a collision hazard in its operational orbit. Collision avoidance maneuvers allow operational satellites to evade this risk; however, evasive maneuvers also result in a temporary mission outage. Moreover, defunct satellites in the operational orbit hasten the accumulation of large and hidden debris fragments, with large fragments inducing additional avoidance maneuvers and hidden fragments representing a catastrophic risk operational satellites cannot avoid. Through these two mechanisms, PMD failures conspire to decrease constellation availability. Availability should also continue to decrease over time as debris accumulates. Because of these dynamics, previous research has shown that PMD reliability is determinative for local collision risk (Swinerd et al., 1999; Radtke et al., 2017). Quick calculations reinforce this point. The low pLEO constellation considered here launches 210 satellites per year. If 10% failed before PMD, this replenishment tempo would introduce 21 defunct satellites into the operational shell each year.

To quantify this impact, we model each constellation assuming a PMD reliability of 0.6 (i.e., the historical industry-wide estimate), 0.9 (i.e., the ODMSP standard), and 0.99 (i.e., ODMSP recommendation for pLEO). For these calculations, we assume an operational satellite will conduct an evasive maneuver to avoid any forecasted conjunction with a 1 km or less miss distance. Further, we assume such a maneuver imparts a 12-hour mission outage.

Table 2 reports constellation availability across 5-, 10-, 25-, and 50-year time horizons. As hypothesized, PMD reliability has a noticeable impact on constellation availability. The results are starkest for the lower altitude constellations. As Figure 2 demonstrates, the 600 km and 800 km altitudes bands are already heavily polluted with debris. This accelerates the accumulation of pLEO debris and the associated impacts on availability. Applying historical PMD compliance to pLEO architectures here makes the lower altitudes of LEO largely unusable for the foreseeable future. Even adhering to the ODMSP standard of 0.9 reduces constellation availability after 25 years to 0.768 and 0.720, respectively. Indeed, in these lower altitudes, the ODMSP recommended reliability of 0.99 is an operational imperative. The medium-high and high constellations are less sensitive to PMD reliability with a 0.9 PMD reliability sufficient to maintain constellation

Table 2. The impact of PMD reliability on constellation availability.

	Constellation availability		
	$\theta = 0.6$ (5 / 10 / 25 / 50 years)	$\theta = 0.9$ (5 / 10 / 25 / 50 years)	$\theta = 0.99$ (5 / 10 / 25 / 50 years)
Low	0.809 / 0.630 / 0.504 / 0.471	0.950 / 0.902 / 0.768 / 0.707	0.970 / 0.956 / 0.927 / 0.919
Medium-low	0.833 / 0.655 / 0.364 / 0.258	0.927 / 0.893 / 0.720 / 0.518	0.941 / 0.933 / 0.906 / 0.851
Medium-high	0.945 / 0.869 / 0.612 / 0.476	0.982 / 0.974 / 0.915 / 0.754	0.987 / 0.986 / 0.982 / 0.971
High	0.966 / 0.920 / 0.713 / 0.566	0.988 / 0.983 / 0.948 / 0.833	0.991 / 0.990 / 0.988 / 0.980

Note. In this table, number of years is measured starting with the initial deployment of a complete constellation (i.e., the number of years after FOC is achieved).

availability above 0.9 for at least 25 years. Because these designs operate at a higher altitude, they require less satellites—and hence generate less debris—while simultaneously operating in a larger volume than the lower constellations.

What design attributes can improve constellation availability? Redundancy and superior reliability for critical PMD subsystems are the most obvious. These types of enhancements would decrease the probability that any satellite would malfunction before ultimate disposal. Active debris removal presents another potential opportunity. By repositioning defunct satellites outside the operational shell, active debris removal serves as a kind of failsafe that retroactively corrects PMD failures. Indeed, improved subsystem reliability, redundancy, and active debris removal all attempt to improve constellation availability by dampening the collision hazard derelict satellites create.

A resiliency strategy, on the other hand, could seek to reduce the mission loss associated with evasive maneuvers. Mission loss duration depends on attitude control performance and mission context, but typically varies from 15 minutes to 24 hours. Figures 4 and 5 explore if reducing COLA mission loss can partially compensate for PMD reliability in the low and medium-low architectures.

The steep slopes in Figure 4 imply that availability in the low constellation is relatively inelastic to changes in COLA loss; here, PMD reliability is determinative. Regardless of COLA maneuver mission loss, the constellation must maintain a PMD compliance between 0.96 and 0.98 to achieve an expected availability greater than 0.90 after 25 years. The results are more nuanced in the medium-low altitude (Figure 5). Here, where congestion is greatest, 0.9 expected constellation availability can be achieved with a PMD reliability as low as 0.941, provided COLA mission loss is limited to a few hours. Conversely, 0.9 expected availability becomes infeasible if COLA mission loss

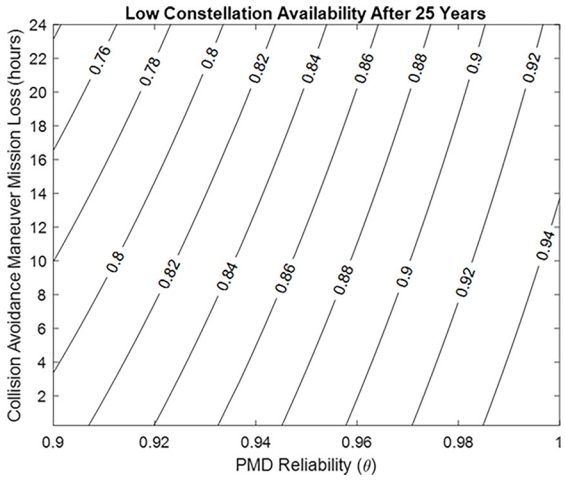

Figure 4. Low constellation availability (mission loss vs. PMD reliability).

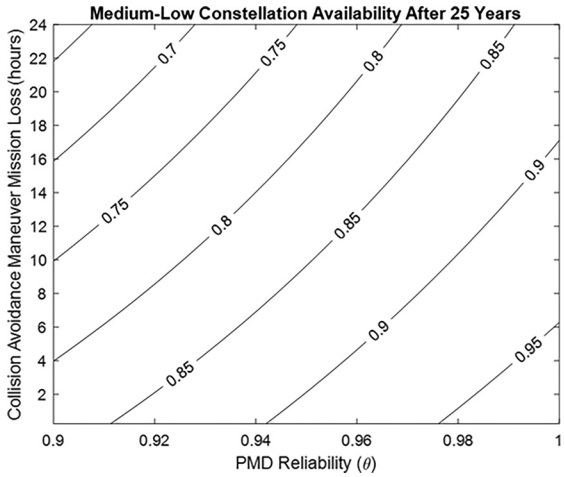

Figure 5. Medium-low constellation availability (mission loss vs. PMD reliability).

exceeds 16 hours. The range of possible outcomes makes COLA mission loss an important design attribute in the medium-low architecture.

Environmental Impact

New pLEO debris is not confined to its initial operational orbit. Instead, gradual atmospheric decay redistributes debris across lower altitudes. Through this mechanism, pLEO constellations will influence the LEO-wide debris environment. This section attempts to quantity that impact over time.

Two competing design choices drive debris generation—constellation size and natural decay timelines. On one hand, comparatively low constellations require more satellites to achieve the same amount of Earth coverage, an attribute that motivates an increase in debris. On the other hand, low altitude debris decays into the atmosphere faster than debris at higher altitudes, an attribute that slows the accumulation of debris.

To understand the net result of these competing forces, we compare the evolution of the LEO debris population for each notional architecture to a baseline scenario. Here, the baseline scenario assumes no pLEO constellations while preserving historical launch rates, ODMSP guidelines, and historical ODMSP compliance rates. Each scenario considers a 100-year period where one of the notional pLEO architectures is active for 50 years, followed by 50 years of inactivity. This design isolates the residual impact of pLEO constellations that persists after the cessation of constellation replenishment. Finally, the results in Figure 6 assume the pLEO constellations achieve 90% compliance with the 25-year PMD disposal requirement.

The low pLEO architecture has the smallest impact on the LEO environment. After 100 years, the low pLEO design imparts a 5.31% increase in the total number of large debris fragments in LEO when compared to the baseline. Even though this constellation requires 210 new satellites per year—73 more per year than the second largest constellation—rapid decay timelines inhibit debris' viscous cycle. Conversely, the medium-low constellation has the largest deleterious impact on the LEO environment, increasing the total debris population by 18.89%. The 800 km altitude acts as a kind of "sweet spot" for debris generation. Unlike the low constellation, decay rates at the medium-low altitude are too slow to offset the comparatively large number of satellites required to achieve comparable coverage. An already congested altitude further exasperates this problem.

To better quantify the net effect of these competing dynamics, we introduce the concept of orbital debris elasticity, ε_{OD}, of a satellite constellation:

$$\varepsilon_{OD} = \frac{\%\Delta\ Orbital\ Debris\ Population}{\%\Delta\ Launch\ Rate}. \tag{18}$$

Table 3 reports orbital debris elasticities for each notional constellation. As an example, consider the low pLEO constellation. The baseline LEO launch rate used in this analysis is 167.3 satellites per year. Assuming 90% compliance with a 25-year PMD standard, the low pLEO design increases the total debris population by 5.31% after 100 years, yielding $\varepsilon_{OD} = 0.04$. Thus, for the low pLEO design with a 50-year operational life, every 1% increase in LEO launch rate yields a 0.04% increase in the total LEO population after 100 years.

As stated earlier, the results in Figure 6 and Table 3 assume each pLEO constellation achieves 90% compliance with a 25-year PMD standard. Can more stringent mitigation noticeably improve total debris accumulation? And if so, what is more important, decreasing PMD timelines or increasing PMD reliability? To answer these questions, we calculate the percent increase in debris accumulation for four mitigation strategies: five-year and 25-year PMD timelines, each with 0.9 and 0.99 PMD reliability. For our calculations, these mitigation standards only apply to the notional military pLEO constellations. Outside this narrow population, 60% compliance with the 25-year rule persists for all other LEO satellite activity.

Table 4 quantifies the effectiveness of different debris mitigation policies. A cursory glance reveals that mitigation can noticeably impact LEO-wide debris accumulation and that PMD compliance, not PMD timeline, is the crucial factor. Should the DOD implement a five-year PMD timeline for any pLEO military satellite, the average effect across the four notional constellations is less than a 1 percentage point decrease in the total LEO debris population over a 100-year time horizon. PMD compliance, on the other hand, has a much larger effect. Increasing PMD reliability from 0.9 to 0.99 for DOD pLEO satellites can decrease the total LEO debris population by as much as 14.98 percentage points over the examined period. It seems clear that maximizing the effectiveness of mitigation efforts means prioritizing increased PMD reliability.

CONCLUDING REMARKS

The stipulations on PMD reliability in ODMSP are likely too lenient for most military-grade applications. Military pLEO architectures must be designed to achieve a constellation-wide PMD reliability that approaches 99%. Such a standard preserves constellation availability while also minimizing the impact on the larger debris environment. Realizing this high standard will likely require a combination of enhanced subsystem redundancy, cautious standard operating

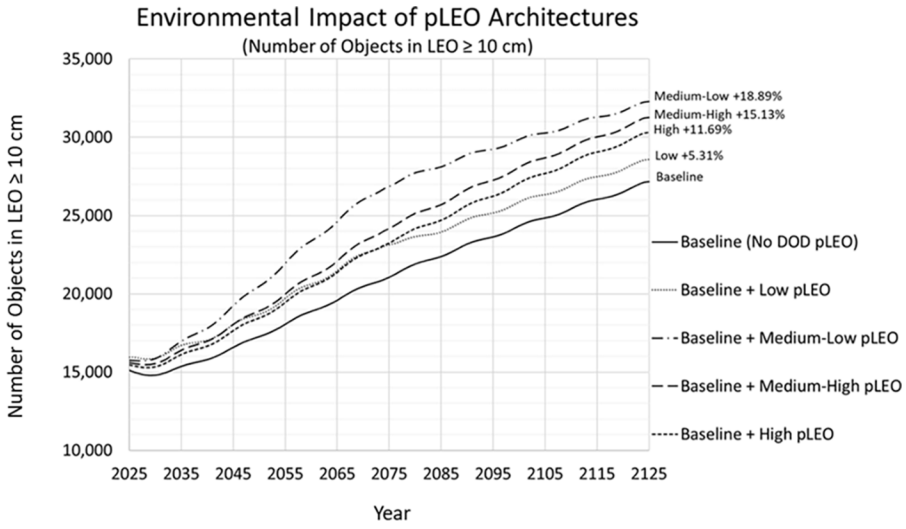

Figure 6. Debris accumulation in LEO.

Table 3. 100-year debris generation elasticities.

	Low	Medium-low	Medium-high	High
Baseline LEO launch rate	167	167	167	167
Constellation launch rate	210	137	100	78
%Δ in launch rate	125.5%	81.9%	59.8%	46.6%
%Δ in large debris fragments (t =100)	5.3%	18.9%	15.1%	11.7%
Orbital debris generation elasticity (ε_{ODG})	0.04	0.23	0.25	0.25

Table 4. Orbital debris mitigation effectiveness.

Percent change in the LEO debris population (≥10cm) resulting from the medium-high design				
Mitigation standards	Low	Medium-low	Medium-high	High
PMD = 25 years, PMD θ = 0.90	5.99%	18.89%	15.13%	11.69%
PMD = 5 years, PMD θ = 0.90	5.31%	18.33%	14.63%	11.30%
PMD = 25 years, PMD θ = 0.99	3.68%	4.04%	7.51%	6.50%
PMD = 5 years, PMD θ = 0.99	2.65%	3.22%	6.86%	6.03%
Factor change (percentage points)	Low	Medium-low	Medium-high	High
PMD: 25 → 5 years	−0.85%	−0.69%	−0.57%	−0.43%
θ: 0.9 → 0.99	−2.48%	−14.98%	−7.69%	−5.23%

procedures, and an active debris removal capability to remediate any malfunctions that preclude disposal. Conversely, reducing the PMD altitude, even substantially from 25 years to five years, has a minimal impact on LEO-wide debris growth. Confronting the debris threat to pLEO involves more than passive mitigation. Constellation resiliency is a function of space traffic management, satellite maneuverability, and attitude control performance. Indeed, debris considerations for pLEO architectures permeate every portion of the space mission design process. Rather than blindly accept ODMSP as "good enough," each DOD pLEO constellation likely requires its own detailed, high-fidelity analysis of collision risk and debris mitigation performance. The research presented here motivates this requirement but lacks the specificity and sophistication necessary to recommend universal debris mitigation design parameters for all DOD pLEO constellations.

PLEO applications will transform the logic of orbital debris mitigation. Since the 1980s, sentiments of long-term sustainability and environmental stewardship have motivated the policy and practice of debris mitigation. This framework implicitly casts debris mitigation as an extrinsic practice that responsible actors undertake to preserve a usable space environment for future generations. To be sure, these long-term considerations persist. But short-term pragmatism now reinforces long-term stewardship.

As this analysis shows, pLEO architectures ignite an urgency for stringent mitigation—especially enhanced PMD reliability—based on the narrow logic of military readiness. Lackadaisical mitigation for pLEO architectures can have a deleterious effect on constellation availability in as little as five years. Even strict adherence to the ODMSP stipulated 90% compliance rate can render constellations lower than 1,000 km unusable in less than 25 years. In pLEO architectures, debris mitigation is intrinsically and inexorably linked to the performance and military readiness of the constellation. This is a short-term, pragmatic consideration that must be incorporated into constellation design early in the requirements process. When analogizing these dynamics, we find one aphorism particularly helpful: "it's an sick bird that fouls its own nest." Unless debris mitigation and debris resiliency are properly addressed early in the design process for military pLEO architectures, "sick-bird syndrome" may cancel the potential benefits of pLEO while also accelerating the dangerous growth of orbital debris across the LEO regime.

AUTHORS' STATEMENT

We would like to thank Professors Brad Holst, Adam Thomas, and Micah Jensen for sharpening our analytical skills and preparing us for the publication process. We would also like to thank Colonel (retired) Jack Fischer and four anonymous reviewers whose feedback enhanced this research and focused our conclusions. The views expressed are those of the authors and do not reflect the official policy or position of the U.S. Air Force, U.S. Space Force, Department of Defense, or the U.S. Government.

REFERENCES

Bradley, A. M., and Wein, L. M. 2009. Space Debris: Assessing Risk and Responsibility, *Advances in Space Research*, Vol 43, No 9, 1372–1390.

Eichler, P., and Rex, D. 1990. Debris Chain Reactions. *Orbital Debris Conference: Technical Issues and Future Directions, AIAA-90-1365*, 1–9.

ESA Space Debris Office. 2019. *ESA's Annual Space Environment Report.* No. GEN-DB-LOG-00271-OPS-SD. Retrieved from https://www.sdo.esoc.esa.int/environment_report/Space_Environment_Report_latest.pdf.

Henning, G. A., Sorge, M. E., Peterson, G. E., Jenkin, A. B., Mains, D., and McVey, J. P. 2019. Parameterizing Large Constellation Post-Mission Disposal Success to Predict the Impact to Future Space Environment, *First International Orbital Debris Conference*, 1–10.

Johnson, N. L., Krisko, P. H., Liou, J.-C., and Anz-Meadow, P. D. 2001. NASA's New Breakup Model of Evolve 4.0, *Advances in Space Research*, Vol 28, No 9, 1377–1384.

Kessler, D. J. 1981. Sources of Orbital Debris and the Projected Environment for Future Spacecraft, *Journal of Spacecraft and Rockets*, Vol 18, No 4, 357–360.

Kessler, D. J. 1991. Collisional Cascading: The Limits of Population Growth in Low Earth Orbit, *Advances in Space Research*, Vol 11, No 12, 63–66.

Kessler, D. J., and Cour-Palais, B. G. 1978. Collision Frequency of Artificial Satellites: The Creation of a Debris Belt, *Journal of Geophysical Research: Space Physics*, Vol 83, No A6, 2637–2646.

Kessler, D. J., Zhang, J., Matney, M. J., Eichler, P., Reynolds, R. C., Anz-Meador, P. D., and Stansbery, E. G. 1996. *A Computer-Based Orbital Debris Environment Model for Spacecraft Design and Observation in Low Earth Orbit.* Technical Memorandum 104825. National Aeronautics and Space Agency.

Kim, R. H., and Paté-Cornell, E. 2019. Managing the Risk of Satellite Collisions. *Military Operations Research*, Vol 24, No 3, 49–72.

Krisko, P. H. 2007. The Predicted Growth of the Low-Earth Orbit Space Debris Environment—An Assessment of Future Risk for Spacecraft. Proceedings of the Institution of Mechanical Engineers, Part G. *Journal of Aerospace Engineering*, Vol 221, No 6, 975–985.

Lewis, H. G. 2019. Understanding Long Term Orbital Debris Population Dynamics. *First International Orbital Debris Conference*, American Institute of Aeronautics and Astronautics, 1–10.

Lewis, H., Radtke, J., Rossi, A., Beck, J., Oswald, M., Anderson, P., and Krag, H. 2017. Sensitivity of the Space Debris Environment to Large Constellations and Small Satellites, *Journal of the British Interplanetary Society*, Vol 70, 105–117.

McKnight, D. S., and Anz-Meadort, P. D. 1993. Historical Growth of Quantities Affecting On-Orbit Collision Hazard, *Journal of Spacecraft and Rockets*, Vol 30, No 1, 120–124.

National Aeronautics and Space Administration (NASA), Orbital Debris Program Office. 2020. Orbital Debris Engineering Model. Accessed on 12 June 2020. https://www.orbitaldebris.jsc.nasa.gov/modeling/engrmodeling.html.

Liou, J.-C. 2011. An Active Debris Removal Parametric Study for LEO Environment Remediation, *Advances in Space Research*, Vol 47, No 11, 1865–1876.

Liou, J.-C. 2020. Risk from Orbital Debris and Space Situational Awareness. National Aeronautics and Space Administration (Orbital Debris Program Office). Retrieved from https://ntrs.nasa.gov/archive/nasa/casi.ntrs.nasa.gov/20200000450.pdf.

Liou, J. C., Hall, D. T., Krisko, P. H., and Opiela, J. N. 2004. LEGEND–A Three-Dimensional LEO-to-GEO Debris Evolutionary Model, *Advances in Space Research*, Vol 34, No 5, 981–986.

Liou, J.-C. and Johnson, N. L. 2006. Risks in Space from Orbiting Debris, *Science*, Vol 311, No 5759, 340–341.

Polk, E., and Roebuck, B. 2015. *DebrisSat Hypervelocity Impact Test*. Final report. Arnold Engineering Development Complex. https://apps.dtic.mil/sti/pdfs/ADA625195.pdf.

Radtke, J., Kebschull, C., and Stoll, E. 2017. Interactions of the Space Debris Environment with Mega Constellations—Using the Example of the OneWeb Constellation, *Acta Astronautica*, Vol 131, 55–68.

Reesman, R., Gleason, M. P., Bryant, L., and Stover, C. 2020. *Slash the Trash: Incentivizing Deorbit*. The Aerospace Corporation. Accessed June 1, 2020, at https://aerospace.org/sites/default/files/2020-04/Reesman_SlashTheTrash_20200422.pdf.

Space Development Agency. 2020. Statement of Work: Space Transport Layer Tranche 0. Solicitation number HQ085020R0001.

Space Exploration Technologies Corporation. 2016. Federal Communications Commission SAT-LOA-20161115-00118. SpaceX Non-geostationary Satellite System: Attachment A Technical Information to Supplement Schedule S. Accessed June 1, 2020, at https://licensing.fcc.gov/myibfs/download.do?attachment_key=1158350.

Su, S. Y. 1986. Orbital Debris Environment Resulting from Future Activities in Space, *Advances in Space Research*, Vol 6, No 7, 109–117.

Su, S. Y., and Kessler, D. J. 1985. Contribution of Explosion and Future Collision Fragments to the Orbital Debris Environment, *Advances in Space Research*, Vol 5, No 2, 25–34.

Swinerd, G. G., Barrows, S. P., and Crowther, R. 1999. Short-term Debris Risk to Large Satellite Constellations, *Journal of Guidance, Control, and Dynamics*, Vol 22, No 2, 291–295.

Weeden, B. 2014. Space Traffic Management: Preventing a Real Life "Gravity." U.S. House of Representatives, 113th United States Congress (2nd Session).

Weeden, B. 2017. US Space Policy, Organizational Incentives, and Orbital Debris Removal, *Space Review* (October 30), https://www.thespacereview.com/article/3361/1.

Wertz, J. R., and Larson, W. 1999. *Space Mission Analysis and Design.* Space Technology Series, third edition. Microcosm Press.

White, A. E., and Lewis, H. G. 2014. The Many Futures of Active Debris Removal, *Acta Astronautica*, Vol 95, 189–197.

Weeden, B. 2020. The United States Is Losing Its Leadership Role in the Fight Against Orbital Debris. *Space Review* (February 24), https://www.thespacereview.com/article/3889/1.

Virgili, B. B., Dolado, J. C., Lewis, H. G., Radtke, J., Krag, H., Revelin, B., Cazaux, C., Colombo, C., Crowther, R., and Metz, M. 2016. Risk to Space Sustainability from Large Constellations of Satellites, *Acta Astronautica*, Vol 126, 154–162.

U.S. Government. 2019. Orbital Debris Mitigation Standard Practices. Retrieved from https://orbitaldebris.jsc.nasa.gov/library/usg_orbital_debris_mitigation_standard_practices_november_2019.pdf.